Mechanical Systems and Signal Processing 181 (2022) 109532

Contents lists available at ScienceDirect

Mechanical Systems and Signal Processing

journal homepage: www.elsevier.com/locate/ymssp

Alternative metrics for design decisions based on separating aleatory and epistemic probabilistic uncertainties

John Hickey *, Robin Langley

Department of Engineering, University of Cambridge, Trumpington Street, CB2 1PZ Cambridge, United Kingdom

ARTICLE INFO

Communicated by John E. Mottershead

Keywords:
Epistemic uncertainty
Aleatory variability
Probability theory
Engineering dynamics

ABSTRACT

There is still much philosophical debate about whether a frequentist or subjective view of probability should be adopted. Some uncertainties (typically aleatory uncertainties) are naturally modelled using a frequentist approach, while others (epistemic uncertainties) are clearly subjective in nature. In light of this it has been argued, for example by the German philosopher Rudolf Carnap, that both potential descriptions of uncertainty should be maintained and treated separately. However, in current engineering practice it is common to make no distinction between these two types of uncertainty. Generally, uncertainty is represented by a single figure or distribution, for example a probability of failure, which incorporates both aleatory and epistemic uncertainties. This paper explores the idea of treating aleatory and epistemic uncertainties separately and proposes alternative metrics –based on the epistemic probability of an aleatory probability - which can potentially provide greater insight for the designer in engineering problems. The metrics are illustrated using two example engineering dynamics problems; the prediction of wind induced accelerations in a tall building and optimizing the design of soundproofing in a car. It is shown that as well as providing further insight on the underlying contributing causes of uncertainty, treating aleatory and epistemic uncertainties as separate quantities, as opposed to in the traditional combined manner, can potentially lead to different design outcomes.

1. Introduction

There is still philosophical debate about the correct interpretation of probability [1]. Two broad interpretations, often termed the frequentist and subjective approaches, are generally presented. The frequentist view defines probability of some event in terms of the relative frequency with which the event tends to occur, while the subjective view defines probability as a measure of the strength of belief regarding the true situation. Various authors have argued that one approach is superior to the other. This debate exists in both classic texts (with 'frequentist' works like those by von Mises or Feller and 'subjectivist' or 'Bayesian' ones such as those by Ramsey or Jaynes) and contemporary literature [2,3]. In his work *Logical Foundations of Probability* [4] the German philosopher Rudolf Carnap argues that both descriptions of probability should be maintained as the frequentist and subjectivist approaches are fundamentally different, or '*there are two fundamentally different concepts for which the term 'probability' is in general use*'. Rather than promoting one view over the other, he argues that '*both concepts are important for science*' and defines two separate types of probability, which he refers to as Probability$_1$ and Probability$_2$:

* Corresponding author.
E-mail address: jmh260@cam.ac.uk (J. Hickey).

https://doi.org/10.1016/j.ymssp.2022.109532
Received 10 January 2022; Received in revised form 27 May 2022; Accepted 3 July 2022
Available online 9 July 2022
0888-3270/© 2022 The Author(s). Published by Elsevier Ltd. This is an open access article under the CC BY license (http://creativecommons.org/licenses/by/4.0/).

(i) Probability$_1$ is the degree of confirmation of a hypothesis h with respect to an evidence statement e, e.g., an observational report.
(ii) Probability$_2$ is the relative frequency (in the long run) of one property of events or things with respect to another.

Both Probability$_1$ and Probability$_2$ are probabilities in the sense that they have a value between 0 and 1 and can be represented by a cumulative distribution function (CDF) or the corresponding probability density function (PDF). The two definitions correspond to the subjective and frequentist views of probability theory respectively. They can also be viewed as the probabilities arising from epistemic uncertainty and aleatory variability. Epistemic uncertainty results from the lack of knowledge about the system of interest. Since it stems from the lack of knowledge, it can be reduced by obtaining additional information. Aleatory variability is the natural variation of inputs that impact outputs of interest. This uncertainty is irreducible.

While on one level this may appear academic or semantic, the destination between the two types of probability is relevant for engineering design. The interpretation of the output of a probabilistic analysis is dependent on the nature of the uncertainties under examination. The result can only be expected to agree with experimental observations if the output is frequentist, or Probability$_2$. Therefore, in principle, identifying the relative contribution of lack of knowledge (i.e., epistemic) uncertainty and inherent (i.e., aleatory) variability on the final results is relevant, especially from a risk management perspective. As epistemic uncertainty can generally be reduced with the additional expenditure of resources, decisions can readily be made with respect to the cost/benefit of such activities [5].

These statements are obvious to a large degree, but nonetheless in practice it is common to combine both types of probability in analysis and interpret the output in a frequentist sense. To pick just one example, in earthquake engineering the FEMA P-58 guide for building performance assessment [6] recommends using a square root sum of squares approach to combine two values for standard deviation representing epistemic uncertainty in structural modelling and aleatory variability in ground motion into a single overall standard deviation value. This combined value is then used to define a distribution representing probable building performance.

However, while it may not be overly common in engineering practice, the separation of aleatory and epistemic uncertainty sources has been examined in many academic studies. Examples of studies where this has been done include [7–10] and many more. Studies of this type are often motivated by the desire to use alternative mathematical representations of aleatory and epistemic uncertainty. While it is widely accepted that aleatory uncertainty is best represented using probability theory, there is more debate about how best to represent epistemic uncertainty (for example [11]). Several alternative mathematical structures are available for this purpose, including interval theory, Dempster-Shafer theory of evidence, fuzzy set theory and possibility theory (see [12] for detailed discussion). Treating epistemic and aleatory uncertainty as separate quantities allows for the development of a family of distributions, each with an uncertainty structure deriving from the particular uncertainty structure used to represent epistemic uncertainty. Plotted together this family, or ensemble, of distributions is sometimes referred to as a 'horsetail' plot [13] where each individual distribution can be referred to as a 'hair'.

There is a more limited body of work where, in line with Carnap's ideas, probability theory is used to represent both epistemic and aleatory uncertainty, but the two probabilities are propagated through the analysis as separate quantities. One notable example where this concept has been applied in an engineering context is the series of works related to the proposed design of the high level radioactive waste repository at Yucca Mountain in Nevada [14–18], which was ultimately never constructed. A key element of the design was determining the expected radiation dose experienced by a 'reasonably maximally exposed individual'. This approach adopted for this calculation employed probability theory to quantify both aleatory and epistemic uncertainties, but treated these two probabilities as separate quantities. The motivation for this was the stipulation by regulators that the designers estimate the radiation dose via a framework that accounted for both and "probability of occurrence" of future radiation events (an aleatory uncertainty) and "uncertainty" related to the modelling of these events (epistemic uncertainty). A number of metrics defined by integrals involving a probability space for aleatory uncertainty and a probability space for epistemic uncertainty were proposed, including the epistemic expectation of an aleatory expectation and the epistemic probability of an aleatory probability, which may be represented as $\mathit{Probability}_1\{\mathit{Probability}_2\}$ in Carnap's notation. The later representation is sometimes termed a second order probability, which may be understood as the probability that the true probability of something has a certain value [19]. However, to the best of the authors' knowledge, this idea has not gained any traction or been implemented in engineering dynamics.

The overarching aim of this work is to demonstrate that separate treatment of the aleatory and epistemic uncertainties, or Probability$_1$ and Proability$_2$, can lead to further insight. This concept is illustrated using two example metrics –based on the epistemic probability of an aleatory probability - which can potentially provide greater insight for the designer in engineering problems. Use of the metrics is demonstrated for two example engineering dynamics problems; the prediction of wind induced accelerations in a tall building and optimizing the design of soundproofing in a car. There is a specific focus on dynamics in this study, but the concepts are potentially applicable to a range of problems across engineering. The potential benefits of separating uncertainties are illustrated via comparison with the alternative approach, where no distinction is made between aleatory and epistemic uncertainties.

Separation of aleatory and epistemic uncertainties, even if they are both treated probabilistically, is especially relevant for Digital Twins compared to 'traditional' design. In 'traditional' design the design phase is often a separate process from the operational life or asset management phase. This means that in many cases the true values for variables considered epistemically uncertain in design are not evaluated. Hence, there is arguably limited benefit in separating uncertainly types in design, as the benefits of this can only be fully exploited if the reducible uncertainty is actually reduced. However, in contrast, one of the primary purposes of a Digital Twin in engineering dynamics is to quantify and reduce epistemic uncertainties [20] through monitoring of the constructed 'physical twin' and updating of the 'digital twin'. Therefore, given that a goal of a digital twin is to reduce epistemic uncertainty, understanding, prior to

monitoring, to what extent uncertainty may be reduced becomes increasingly beneficial as design decisions, or even the decision as to whether or not to employ a digital twin, may depend on the balance between reducible and irreducible uncertainty.

2. Theory

2.1. Second order failure Probability: $P_1[P_2(fail)]$

Fig. 1 presents a typical engineering problem with associated uncertainty. There is a calculation model with some inputs, x, that are p_1, uncertain (subjective or epistemic) and others, y, that are p_2, uncertain (frequentist or aleatory). It is assumed in this study that these uncertain inputs can be represented by probability density functions $p_1(x)$ and $p_2(y)$ respectively, in line with Carnap's definitions of Probability$_1$ and Probability$_2$. The output of the calculation model is labelled z and has an associated failure level, z_f.

Conventionally, where no distinction is made between probability types, the failure probability in such a scenario is calculated as:

$$P_0(z > z_f|x,y) = \iint_{R(z>z_f)} p_{1,2}(x,y)\mathrm{d}x\mathrm{d}y \tag{1}$$

$R(z > z_f)$, which is the region in x, y space where the output, z, exceeds the allowable level, z_f and $p_{1,2}(x,y)$ is the joint PDF of the input variables. As per standard convention, in this study a lowercase p refers to a probability density function (PDF) while an uppercase P refers to a probability value or cumulative distribution function (CDF).

The calculation described by Eq. (1) makes no distinction between uncertainty types. For the purpose of this paper, this type of combined failure probability is termed P_0, in order to distinguish it from an epistemic, or Probability$_1$, type probability, P_1, or a aleatory, or Probability$_2$, type probability, P_2. An example application of Eq. (1), which may provide further clarity, is presented in Section 3 of this paper and illustrated in Fig. 5.

An alternative to this combined P_0 failure probability can be obtained by treating epistemic and aleatory uncertainties as separate quantities. A metric for this purpose is proposed in Eqs. (2) and (3). This a two-step calculation process, where aleatory failure probability conditional on the epistemic variables is calculated first, before the epistemic probability of this being the case is evaluated. The first step involves obtaining the conditional probability of failure given a value of x, which can be done as follows:

$$P_2(z > z_f|x) = \int_{R_1(z>z_f|x)} p_2(y)\mathrm{d}y \tag{2}$$

where R_1 is the region of y values where the output, z, exceeds the allowable level, z_f for a given x. This calculation can be repeated for all possible values of x, allowing a conditional distribution to be developed. The second step involves establishing an acceptable P_2 failure probability, denoted $\widehat{P}_2$, for example $\widehat{P}_2 = 10\%$, and calculating the P_1 probability of the system being such that this is exceeded:

$$P_1\left[P_2(z > z_f|x) \rangle \widehat{P}_2\right] = \int_{R_2\left(P_2(z>z_f|x)\rangle\widehat{P}_2\right)} p_1(x)\mathrm{d}x \tag{3}$$

where R_2 is the region of x values where the P_2 failure probability, $P_2(z > z_f|x)$, exceeds the acceptable level, $\widehat{P}_2$. This means that instead of a single figure for P_0 failure probability, uncertainty is represented by a second order probability $P_1[P_2]$, which can be used to provide the designer with further insight on the relative contribution of reducible and irreducible uncertainty. An example application of Eqs. (2) and (3), which may provide further clarity, is presented in Figs. 6–8.

This metric, and related measures of median and average values, have previously been proposed by [14]. However, to the best of

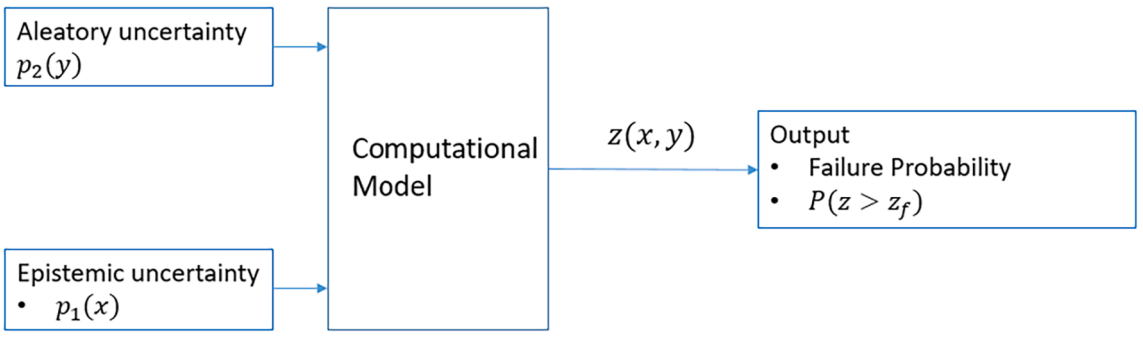

Fig. 1. Typical engineering problem with input parameters with P_1 and P_2 uncertainties.

the author's knowledge, the metric appears to have gained little traction in literature outside of work in the field of nuclear engineering but has importance for use in dynamics, particularly in the context of digital twin accompanied design and asset management.

2.2. Minimization of a cost function

Fig. 2 presents a second typical engineering design problem, this time where a design parameter, η, is selected to minimize some cost function, C, which is a function of the conditional P_2 failure probability for a given η and x, i.e. $C\left(P_2\left(z > z_f|\eta, x\right)\right)$. The aim of the calculation described in this section is to choose an optimal design parameter, η.

There are two ways the optimum design parameter can be selected. Firstly, the expected value, or ensemble average of the cost function, C, can be minimised, as in conventional optimization:

$$\frac{\partial E[C|\eta]}{\partial \eta} = 0 \tag{4}$$

where the expected value of the cost for a given η across the range of possible values of x is obtained by:

$$E[C|\eta] = \int_{-\infty}^{\infty} C\left(P_2\left(z > z_f|\eta, x\right)\right) p_1(x) dx \tag{5}$$

It can be appreciated that the result of Eq. (5) is a function of both probability types and therefore the minimization in Eq. (4) makes no distinction between Probability$_1$ and Probability$_2$. An example application of Eqs. (4) and (5) is presented later in this paper in Section 4 and illustrated in Fig. 16.

Instead of choosing η to minimise $E[C]$, it is possible to define a maximum acceptable cost, $\widehat{c}$, and search for the design parameter value, η, that minimises the P_1 probability of exceeding this cost, $P_1\left[C\left(P_2\left(z > z_f|\eta, x\right)\right) \rangle \widehat{c}\right]$.

The probability of exceeding a maximum acceptable cost, $P_1[C > \widehat{c}]$, is given by:

$$P_1\left[C\left(P_2\left(z > z_f|\eta, x\right)\right) \rangle \widehat{c}\right] = \int_{R_3(C > \widehat{c})} p_1(x) dx \tag{6}$$

where R_3 is the region in the epistemic probability space, or set of values of x, where the cost exceeds the limiting value. The optimum design parameter to minimise this probability can be obtained by conventional minimisation:

$$\frac{\partial P_1\left[C\left(P_2\left(z > z_f|\eta, x\right)\right) \rangle \widehat{c}\right]}{\partial \eta} = 0 \tag{7}$$

An example application of Eqs. (6) and (7) is illustrated schematically in Fig. 15. Unlike Eq. (5), this is a two-step process where the P_2 and P_1 uncertainties are propagated separately. The optimum η value returned by Eq. (7) can be viewed as an alternative to the value returned via Eq. (5). It can also be seen that Eqs. (6) and (7) are based on a cost function. Therefore any computational method whose outputs can be used to define some cost function (for example the Finite Element Method, Stochastic Finite Element Method or Statistical Energy Analysis) can be employed within this framework.

3. Metric 1: Epistemic probability of an aleatory Probability: $P_1[P_2]$

3.1. Illustrative example – Wind induced acceleration of a tall building

In order to illustrate the use of the second order probability metric defined in Eq. (3), the problem of predicting the peak floor acceleration, $\ddot{z}$, of a tall building under wind gusting is considered. This is an applicable example problem as there is clear aleatory uncertainty associated with the wind excitation, while epistemic uncertainty is generally present in the level of damping, which in real-

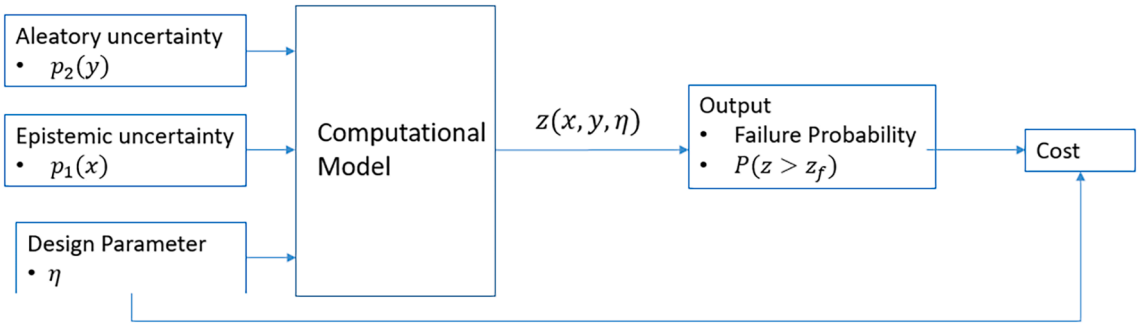

Fig. 2. Typical minimization problem with parameters with P_1 uncertain input and P_2 uncertain failure probability.

world scenarios is often unknown until it is measured after the building is completed. This kind of epistemic uncertainty, where damping is only known after construction, is relatively common in one-off civil engineering structures like tall buildings or pedestrian footbridges [21,22]. Furthermore, there is a clearly defined maximum allowable floor acceleration, $\ddot{z}_f$, specified by ISO 10137:2007 [23]. Accurate calculation of peak floor acceleration of a tall building is difficult, and in reality typically involves wind tunnel testing, but for the purpose of this illustrative example it is assumed that the prediction method proposed in Annex C of the Eurocode 1991-1-4 [24] is adequate for calculating peak along-wind acceleration. Details of this computational model can be found in [25]. Fig. 3 illustrates how this example problem fits neatly in the general calculation framework given in Fig. 1.

The input PDFs for the example case considered are shown in Fig. 4. A normal distribution is employed to represent the subjective uncertainty associated with the level of damping and a Gumbell distribution is used to represent the p_2 probability of the mean 10-minute wind speed. It is important to state that the distribution employed to represent damping is purely illustrative and is not necessarily the optimal way to represent this uncertainty in reality. Any probability distribution, for example a uniform distribution or a lognormal distribution, may be employed within the framework. Appendix A examines the impact of employing a uniform distribution, as opposed to normal distribution, to represent uncertainty in the value for damping in this example problem. However, due to the many different forms of probability distributions that could potentially be employed, and the fact that different example problems will have different sensitivities to the epistemically uncertain parameter, it important to emphasise that it is not possible to make universally applicable statements about the impact of the choice of distribution on the outcome. The joint PDF of these two probability distributions (which assumes that they are not fundamentally different and it is permissible to combine them) is also shown in Fig. 4.

The example building under assessment is assumed to have a natural frequency of 0.3 Hz, which approximately corresponds to a 130 m tall structure. The Eurocode computational model is used to develop a response surface, as illustrated in Fig. 5. In this example, this is done by evaluating the peak acceleration across the entire range of feasible wind speed and damping values, however in (realistic) cases where the computational model is more expensive adopting a more sophisticated sampling approach may be necessary. This is discussed in more detail by [15]. From this response surface, the region where peak acceleration exceeds the allowable limit, R_1, can easily by established, as illustrated in Fig. 5. The P_0 failure probability can then be calculated by numerical integration of the joint PDF of the two input variables over this region, in line with Eq. (1). For this example case, it can be seen that there is a failure probability of 46%. It should be pointed out here that such a high failure probability is realistic as excessive wind induced acceleration is a serviceability failure, where some occupants may feel uncomfortable, as opposed to a critical or ultimate limit state failure leading to building collapse.

The approach described by Eqs. (2) and (3), where Probability_1 and Probability_2 are treated separately, is then considered. Firstly, the conditional failure P_2 failure probability is calculated via Eq. (2), as illustrated in Fig. 6. For a specified damping level, the wind speed where response exceeds the allowable value for peak acceleration, R_1, is identified and the probability of wind speed being in that region is calculated through numerical integration of the p_2 PDF over this region.

Fig. 6 illustrates this calculation of for a damping value of $\zeta = 1.2\%$. It can be seen that for this example scenario, the conditional P_2 failure probability is 44%. The calculation can be repeated across a range of feasible levels of damping, to give a curve showing how the P_2 failure probability changes with damping, $P_2\left(\ddot{z} > \ddot{z}_f|\zeta\right)$, as shown in Fig. 7. The value for $\zeta = 1.2\%$, obtained from the calculation shown in Fig. 6, is marked on the plot, illustrating that Fig. 7 is constructed from repeating this calculation for all feasible value of damping.

This curve, which shows the conditional P_2 probability of failure for a given damping, is the starting point for Eq. (3), where the P_1 probability of damping is considered. In Eq. (3) this is done using a target failure probability, $\widehat{P}_2$. This concept is illustrated in Fig. 8 using a target value of $\widehat{P}_2 = 50\%$. The range of damping values where the conditional P_2 probability of failure is greater than this target value, termed R_2 in Eq. (3), is easily identifiable. The probability of damping corresponding to the this region is then obtained by integrating the PDF of damping, $p_1(\zeta)$, over this region. In the example case shown, there is a 29% P_1 probability that the P_2 failure probability is greater than 50%. Or, phrased slightly differently, there is a 29% P_1 probability that the building will be such that chance of failure due to random excitation exceeds 50%.

A further extension can be made to Eq. (3) at this point. Rather than focus on a single target failure probability, $\widehat{P}_2$, Eq. (3) can be applied across all feasible values of $P_2(\ddot{z} > \ddot{z}_f|\zeta)$, i.e. from 0 to 1. This allows a complimentary CDF (C-CDF) of $P_1[P_2(\ddot{z} > \ddot{z}_f)]$ to be

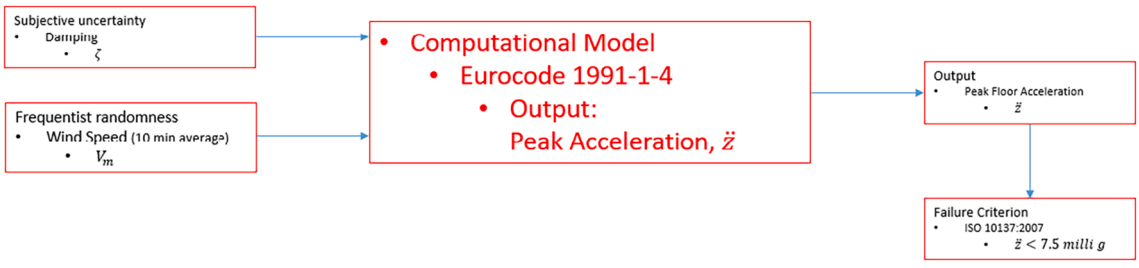

Fig. 3. Application of the framework outlined in Fig. 1 for the wind induced acceleration of a tall building.

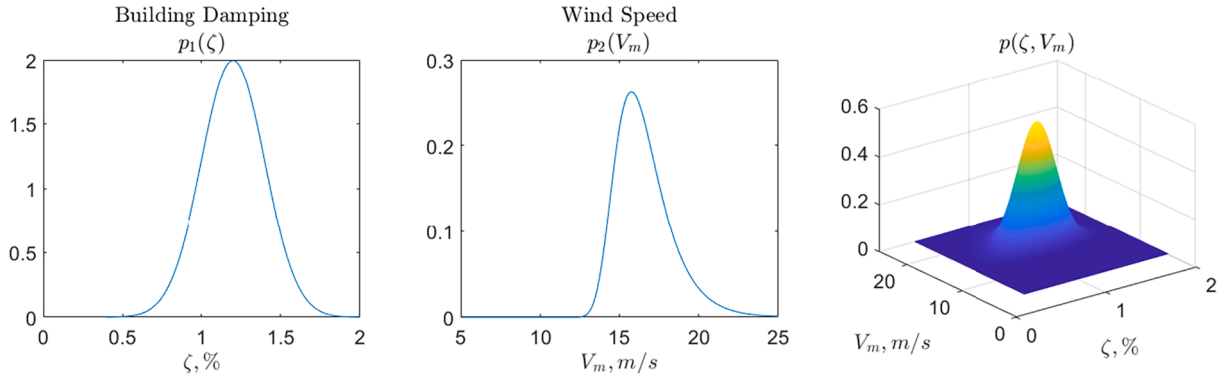

Fig. 4. Input p_1 pdf for damping, p_2 pdf for wind speed and joint pdf if uncertainties are treated together.

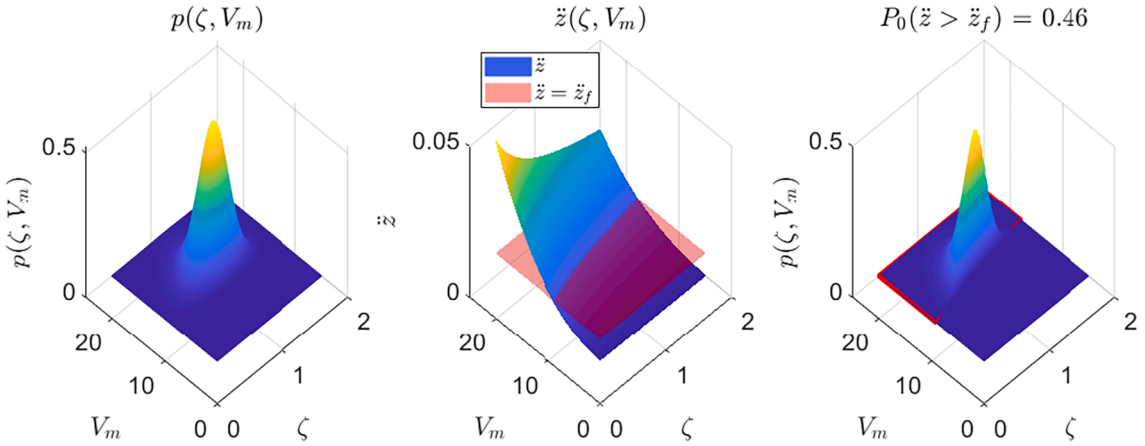

Fig. 5. Illustration of the calculation described by Eq. (1): joint pdf of damping and wind speed; response of the probability space and identification of failure region; integration of the joint pdf of damping and wind speed over failure region to obtain the P_0 failure probability.

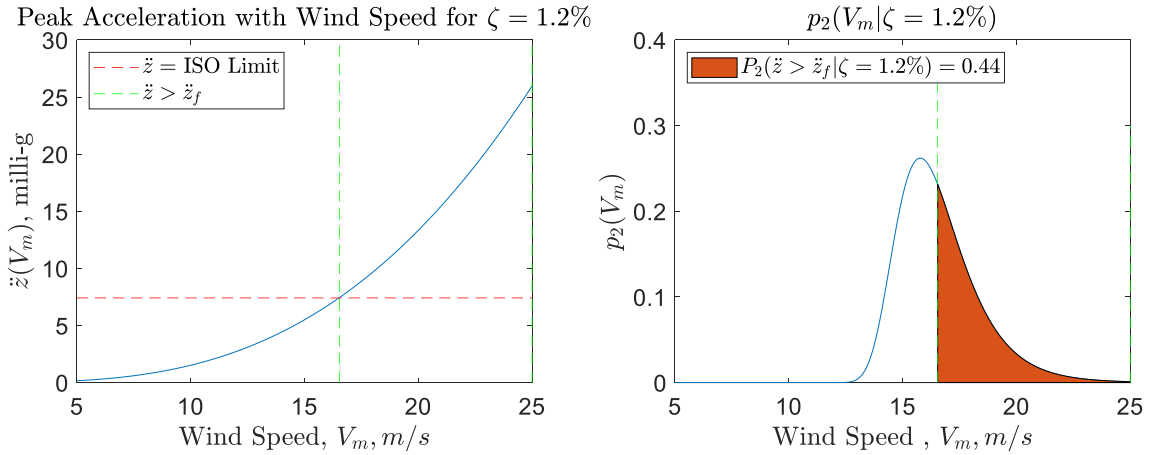

Fig. 6. Example calculation of conditional P_2 failure probability as per Eq. (2) for $\zeta = 1.2\%$; Identification of failure region and calculation of $P_2(\ddot{x}|\zeta)$ failure probability.

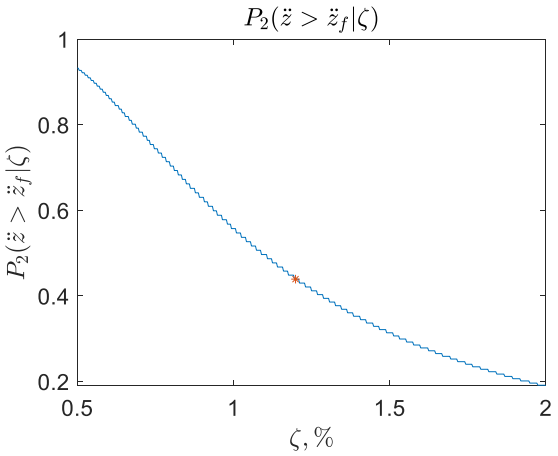

Fig. 7. Conditional $P_2(\text{fail}|\zeta)$ failure probability as per Eq. (2) across a range of damping values.

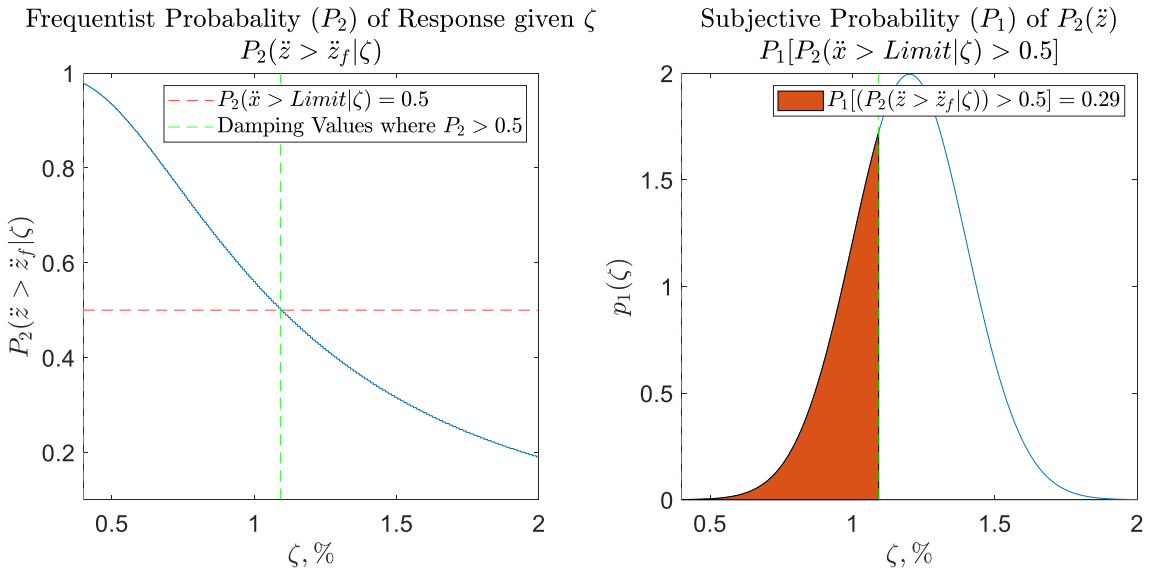

Fig. 8. Illustration of the calculation described by Eq. (3) for $\widehat{P}_2 = 0.5$: identification of the region where $P_2(\text{fail}|\zeta) > \widehat{P}_2$ and calculation of second order failure probability..$P_1[P_2(\text{fail}|\zeta) > \widehat{P}_2]$

constructed, as illustrated in Fig. 9. The value at $\widehat{P}_2 = 50\%$ is marked with an orange dot, again demonstrating how the C-CDF is constructed by simply repeating the calculation performed in Fig. 8 across a range of $\widehat{P}_2$ values.

The $P_1[P_2\left(\ddot{z} > \ddot{z}_f\right)\rangle\widehat{P}_2]$ metric and the C-CDF shown in Fig. 9 are potentially useful tools that can provide further insight for the designer beyond the P_0 failure probability shown in Fig. 5. For example, in the specific case of design of a tall building, if there is a chance of failure, the designer, broadly speaking, has two options. Firstly, they can fundamentally change the design to reduce the probability of failure, for example though altering the building shape or stiffness. Alternatively, they can decide to proceed with the initial design and accept there is a possibility of failure which may need to be addressed with some remedial action post construction, for example through the installation of a tuned mass damper. If a digital twin is employed, the true value of damping can be calculated using measurements from the physical twin. Understanding, prior to these measurements, the contributions of aleatory and epistemic uncertainty to the failure probability, and how likely the probability of failure is to change once the true damping value for finished building is obtained from the digital-physical twin pair, allows the risk of proceeding with a particular design to assessed from an informed position.

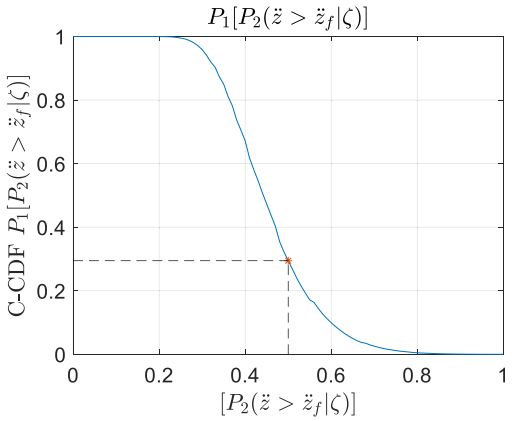

Fig. 9. Complimentary CDF of..$P_1[P_2(\ddot{z} > \ddot{z}_f)]$

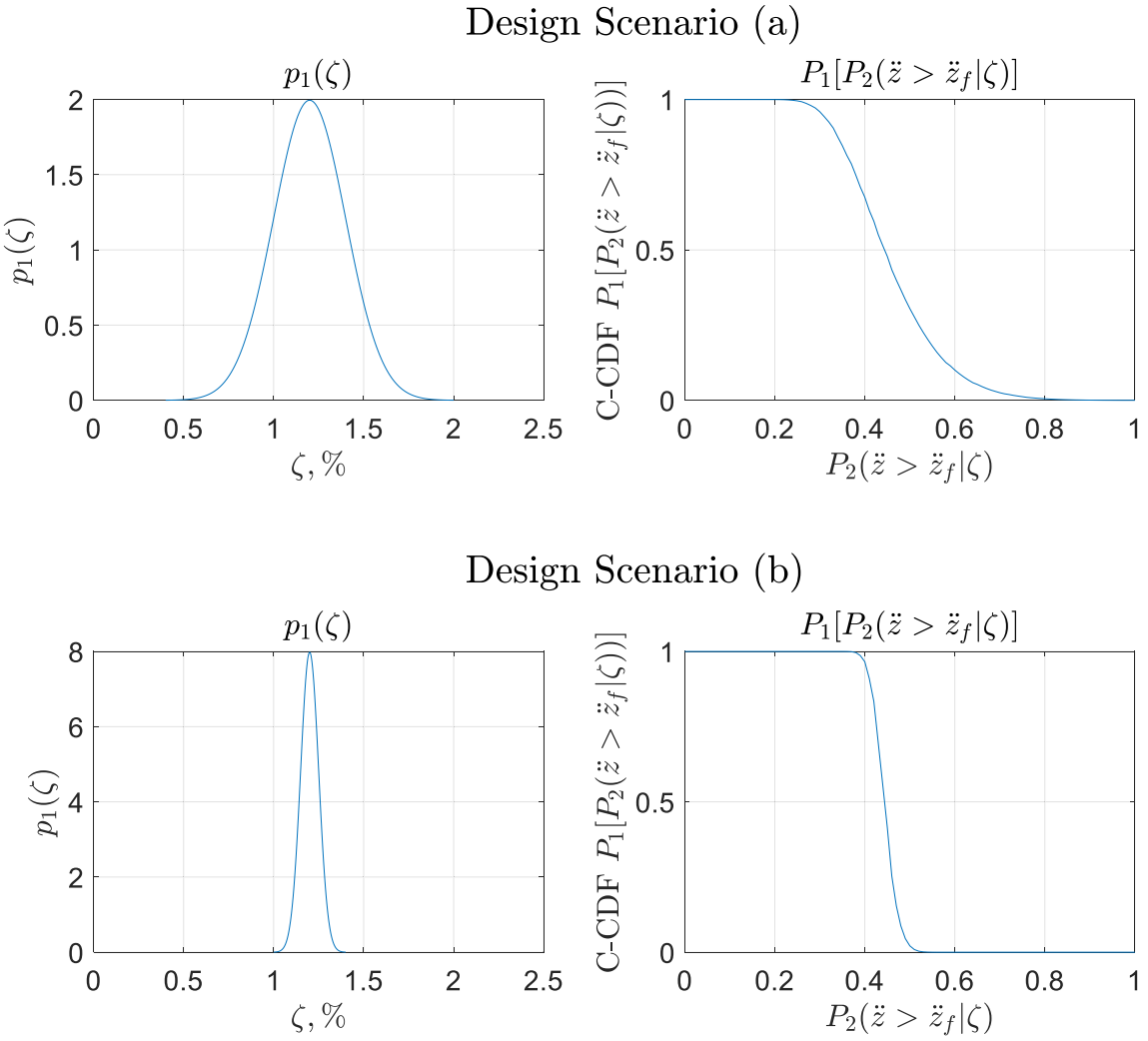

Fig. 10. Example of a C-CDF of $P_1[P_2(\text{fail})]$ for two different design scenarios; one (Design Scenario a) in a case of relatively large epistemic uncertainty and another (Design Scenario b) in a case of relatively small epistemic uncertainty.

3.2. Further discussion of complimentary CDF of $P_1[P_2(fail) > \widehat{P}_2]$

There are a number of additional points worth making about this C-CDF. Firstly, the shape of the curve can inform the designer about the contribution of different uncertainties. This is illustrated in Fig. 10, which shows the CCDF for a two example design scenarios with different levels of epistemic uncertainty associated with damping. It can be seen that for the case of small epistemic uncertainty (achievable if, for example, data is available from an existing similar structure), the C-CDF becomes steeper, or viewed slightly differently, the P_2 failure probability becomes closer to having a fixed deterministic value. In terms of a digital twin, in the case labelled 'Design Scenario (a)', a wide range of failure probabilities (approximately 15% to 100%) appear possible, and learning the true value ζ from measurements on the physical twin will significantly enhance understanding of the structure's future behaviour. In contrast for the scenario labelled 'Design Scenario (b)', the designer knows that the true failure probability is close to 50% and only a limited reduction in uncertainty is achievable from physical twin measurements.

Fig. 11 presents a slightly different example, showing the evolution of the state of knowledge about a single building over time in a digital twin-physical twin pair. This shows the state of the state of knowledge prior to any measurements, and the knowledge after a series of measurements from the physical twin are used to update distribution representing ζ in the digital twin. Given the initial state of knowledge at the in the example shown, the cost/benefit of remedial action is difficult to assess. However, it can be appreciated that in a hypothetical case such as that illustrated, where measurements on the physical twin indicate that damping is lower and P_2 failure probability is higher than initially anticipated, remedial action is likely to be to required to reduce the failure probability.

In addition to this, it is also interesting to note that it can be shown that the area enclosed by the C-CDF is equal to the P_0 probability of failure calculated via Eq. (1) and illustrated in Fig. 5. In other words, for the example problem above, the area under the C-CDF in Fig. 9 is equal to the P_0 failure probability of 0.46 shown in Fig. 5. The proof of this presented in Appendix B.

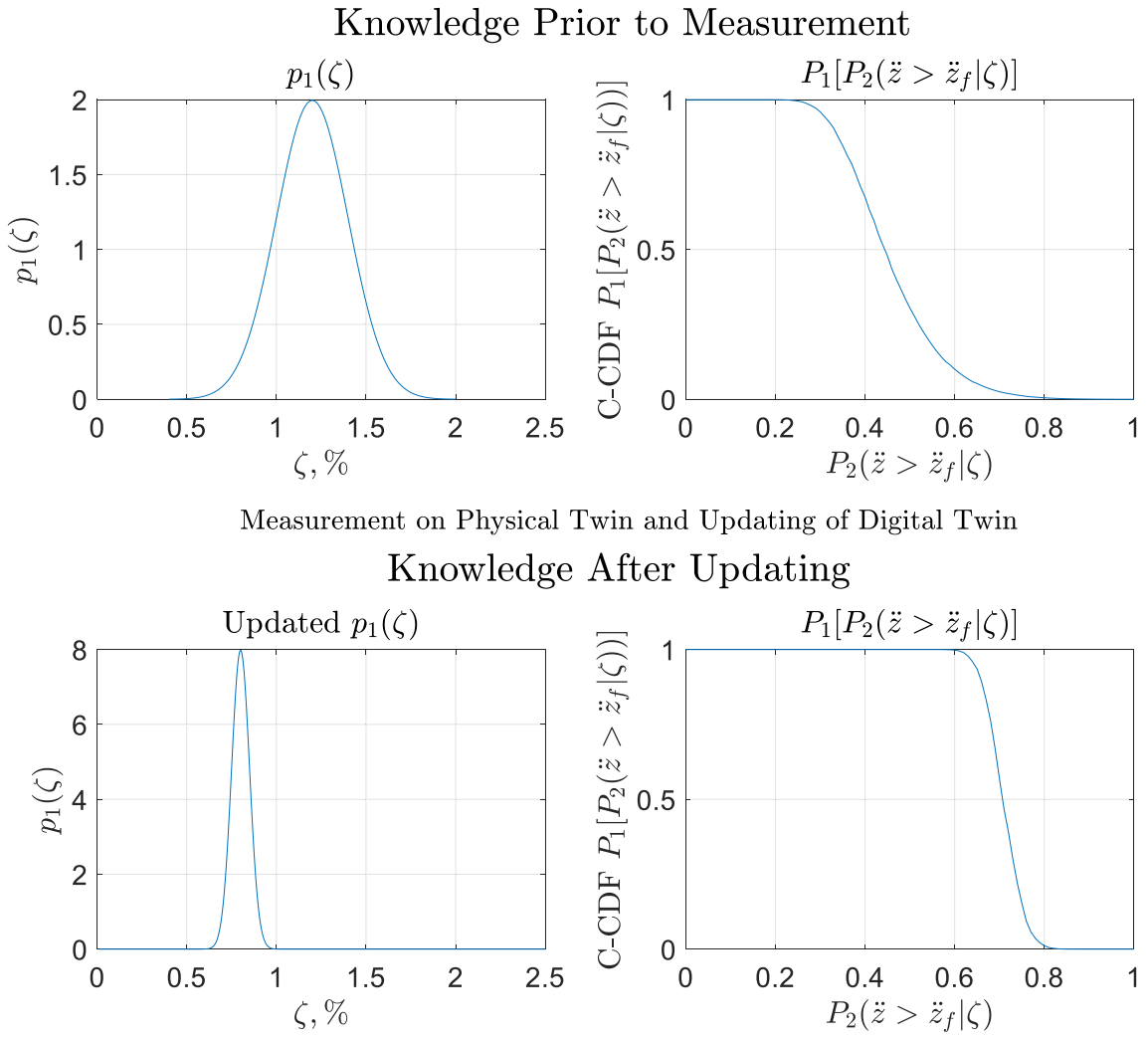

Fig. 11. Example of the evolution of the C-CDF of $P_1[P_2(\text{fail})]$ over time in a digital twin-physical twin pair.

4. Metric 2: Optimized design Parameter η_{opt}

4.1. Illustrative example

The example problem of selecting the optimum level of sound proofing in a car is chosen to demonstrate the application of the metric proposed in Eq. (7). There is both aleatory and epistemic uncertainty associated with the acoustic performance of a car. In terms of aleatory uncertainty, it has been shown that there can be a large differences in the interior noise levels in nominally identical vehicles arising from small variations introduced during the manufacturing process [26,27], for example due to spot weld stiffness which can be different for every vehicle [28]. There is also epistemic uncertainty in production associated with the properties of the production line. This can arise through jig misalignment for example, where the extent of the misalignment is constant but unknown.

The presence of aleatory uncertainty means that for a given production line there is a realizable ensemble of random structures (i.e. cars) that may be produced and therefore the frequency response function of interior sound is P_2 uncertain for each car from that production line. The epistemic uncertainty can be thought of as an unrealizable or imaginary ensemble of production lines, only one of which will exist in reality. As illustrated graphically in Fig. 12, this results in an ensemble of distributions describing the P_2 probability of failure. Failure is deemed to occur when the spatial average of mean squared sound pressure within the cabin of a car under prescribed excitation (for example a shaker at a suspension mount), z, exceeds a limiting value, z_f. The role of the designer is to optimize the level of sound proofing in the car to prevent this limiting value being exceeded whilst minimising the cost of this sound proofing.

For the purpose of this example, calculation of interior noise is performed using a simplistic model to estimate interior sound pressure. Using Statistical Energy Analysis [29], the average z value across an ensemble of random systems (in this case cars), μ_z, can be shown to be inversely proportional to the loss factor of the interior, η such that:

$$\mu_z = \frac{x}{\eta} \tag{8}$$

In terms of design, the engineer controls the level of sound proofing and thus controls η. In this simplified example, it is assumed that x is a variable with some associated epistemic uncertainty arising from a lack of knowledge about the production line, for example in jig alignment or material properties. Given that this is constant but unknown, all cars from a single production line have the same value of x.

Furthermore, it has been shown that a Gaussian Orthogonal Ensemble (GOE) statistical model can be used to quantify natural frequencies across an ensemble of random structures (for example [30,31]). Using a GOE approach, variance, σ_z^2, of the sound pressure can be written as [27]:

$$\frac{\sigma_z^2}{\mu_z^2} = \frac{1}{\pi m} \tag{9}$$

where m is the modal overlap factor, given by:

$$m = \omega n \eta \tag{10}$$

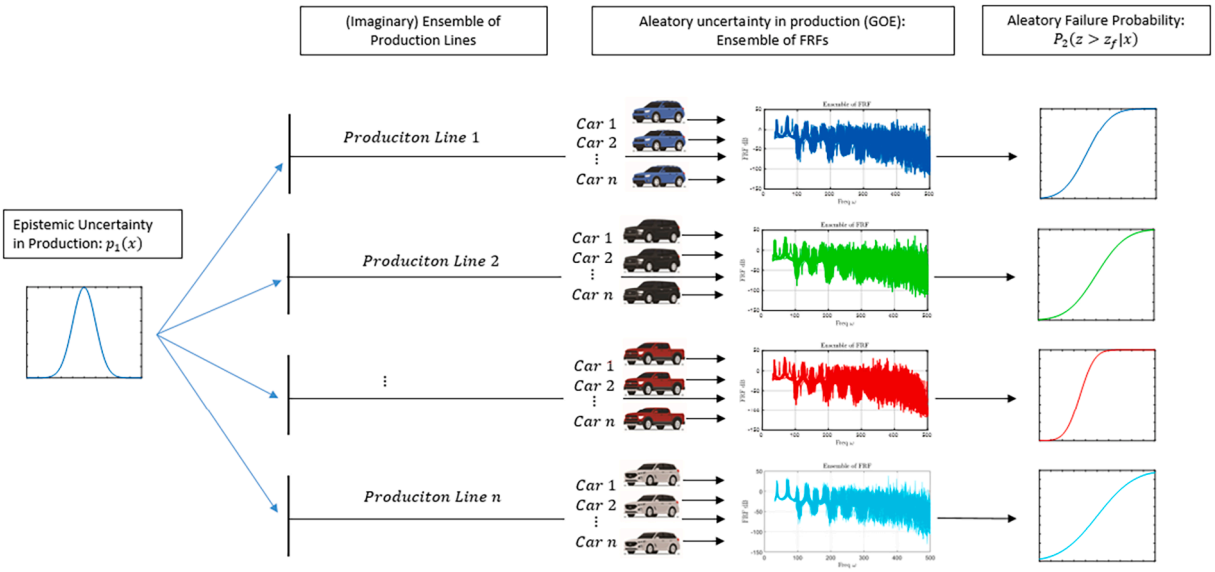

Fig. 12. Illustration of the epistemic and aleatory uncertainties in the example problem of sound-proofing in a car.

where ω is the natural frequency of interest and n is the modal density. Using μ_z and σ_z a p_2 lognormal distribution (which has been shown to be adequate for representing response of systems conforming to GOE [32]) for the mean square sound pressure, conditional on x and η $p_2(z|x,\eta)$, can be constructed. From this the P_2 probability of exceeding a failure threshold z_f, $P_2(z > z_f|x,\eta)$ can be calculated.

For the example problem considered here, the modal density is assumed to equal 50 s and x is assumed to be normally distributed with a mean value of $3 \times 10^{-4}\ N^2/m^4$ and a standard deviation of $1.5 \times 10^{-4} N^2/m^4$. The goal of the design is to keep the spatially averaged interior mean squared sound pressure below 65 dB, i.e. 65 dB is the assumed failure threshold z_f.

As with the tall building example in the previous section, this calculation model is a gross simplification. In reality, a detailed Hybrid Finite Element SEA [33] model of the car would be employed to calculate interior sound pressure, however the simplistic approach described by Eqs. (8) and (9) is adequate to illustrate the optimization procedure.

Fig. 13 shows how the framework shown in Fig. 2 can be applied to this problem. To implement the minimization defined by Eqs. (4) and (7), the cost of production is defined as:

$$C \equiv \alpha\eta + \beta P_2(z > z_f|x,\eta) \tag{11}$$

where α is the unit cost of sound proofing and β is the cost of repairing a failure case. $P_2(z > z_f|x,\eta)$ is the frequentist, or P_2 or aleatory, probability of failure for given x and η. Eq. (18) employs the law of large numbers, and therefore is suitable only for a scenario where a large number of units are produced, like a car production line, as opposed to a one-off structure like a tall building.

Substituting Eq. (11) into Eq. (4), the optimum η value to minimise the expected cost, i.e. the optimum value with no separation of uncertainty types, is given by:

$$\frac{\partial}{\partial\eta}\left\{\int_{-\infty}^{\infty}\left[\alpha\eta + \beta P_2(z > z_f|x,\eta)\right]p_1(x)dx\right\} = 0 \tag{12}$$

Fig. 14 illustrates this calculation for $\beta = 150\alpha$. It can be observed that in this case the optimum value for η is 0.09.

Alternatively, as outlined by Eqs. (6) and (7), η can be selected to minimise the P_1 probability of exceeding a limiting cost, $\hat{c}$. Fig. 15 illustrates the implementation of this process with the acceptable cost (arbitrarily) set to 60 and, as in Fig. 16, $\beta = 150\alpha$. Firstly, the region where the cost function exceeds the maximum acceptable cost is identified, as shown in the plot on the left, before the P_1 probability of this value being exceeded for each η is calculated by numerically integrating $p_1(x)$ over this region. Doing this for each value of η allows a curve showing $P_1[C > \hat{c}]$ as a function of η to be developed, as shown by the plot on the right. From this, an optimum value, which in this example case is $\eta = 0.07$, can be identified.

4.2. Difference in optimum value between approaches

Through some relatively straight forward manipulation of Eq. (12), it can be shown that when $E[C]$ is minimised, i.e. when no distinction is made between the uncertainty types, the optimum η value satisfies the equation:

$$\frac{\alpha}{\beta} = -\frac{\partial}{\partial\eta}\left[\int_{-\infty}^{\infty} P_2(z > z_f|\eta,x)p(x)dx\right] \tag{13}$$

Similarly, through a combination of Eq. (6), 7 and 11, it can be shown that when $P_1[C > \hat{c}]$ is minimised, i.e. when the uncertainty types are treated separately, the optimum design η value satisfies the equation:

$$\frac{\alpha}{\beta} = \frac{-1}{\int_{R_3} p(x)dx}\frac{\partial}{\partial\eta}\left[\int_{R_3} P_2(z > z_f|\eta,x)p(x)dx\right] \tag{14}$$

Comparing of Eq. (13) and Eq. (14), it can be appreciated that the optimum design parameter from the two approaches is different, and will only be the same if the region R_3 ranges from $-\infty$ to ∞, or in practical terms covers the entire range of feasible values of x. For practical implementation, it is not necessary to evaluate the derivatives in Eq. (13) or (14). These Equations are presented simply to

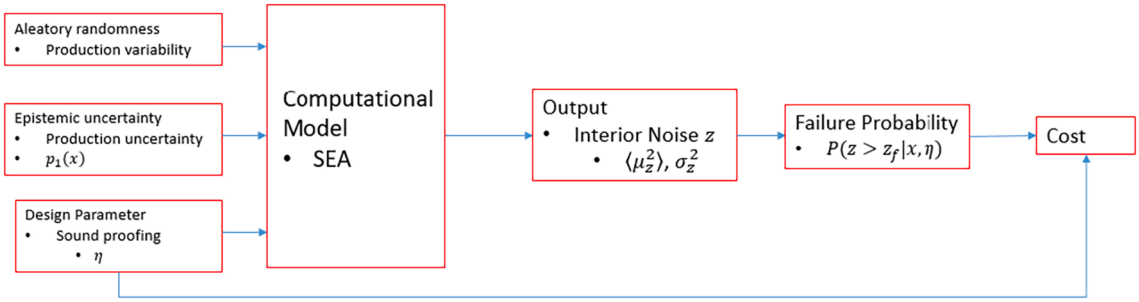

Fig. 13. Application of the framework outlined in Fig. 2 for selection of the optimum level of sound proofing in a car.

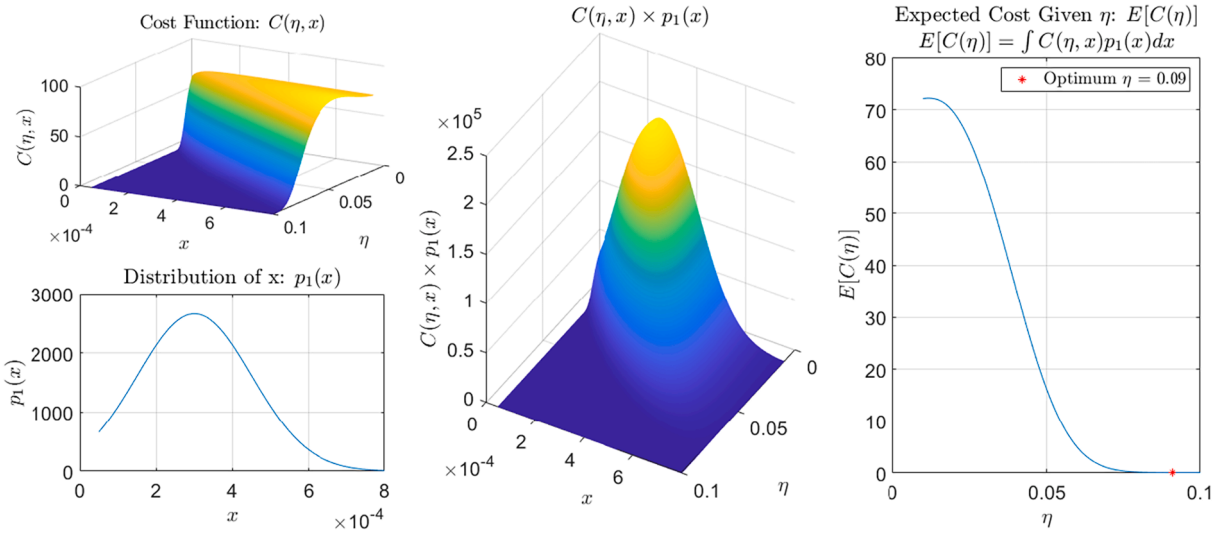

Fig. 14. Illustration of the calculation described by Eq. (12) showing the cost function, $p_1(x)$ and..E[C(η)]

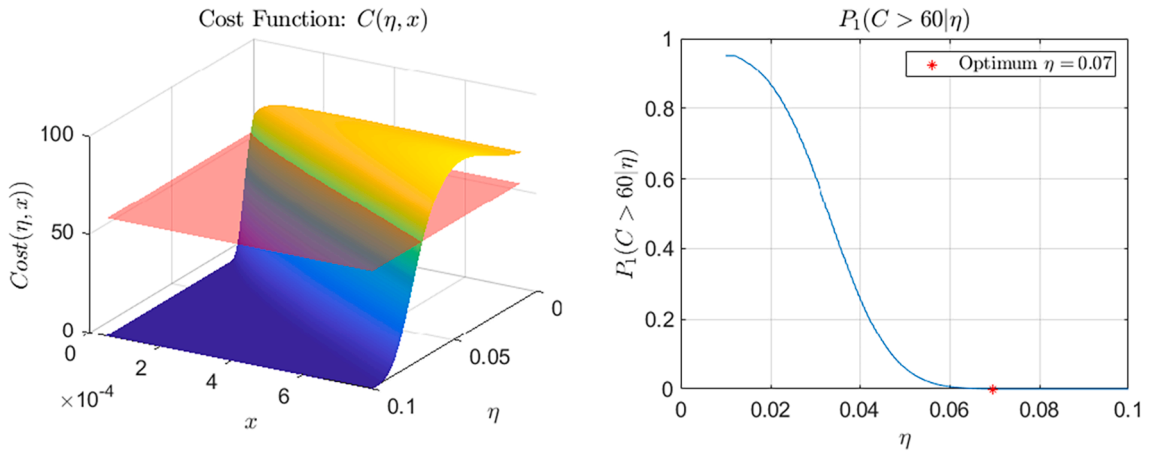

Fig. 15. Illustration of the calculation process described by Eqs. (6) and (7), showing the cost function, limiting cost and P_1 probability of cost exceeding the limiting cost for given η values.

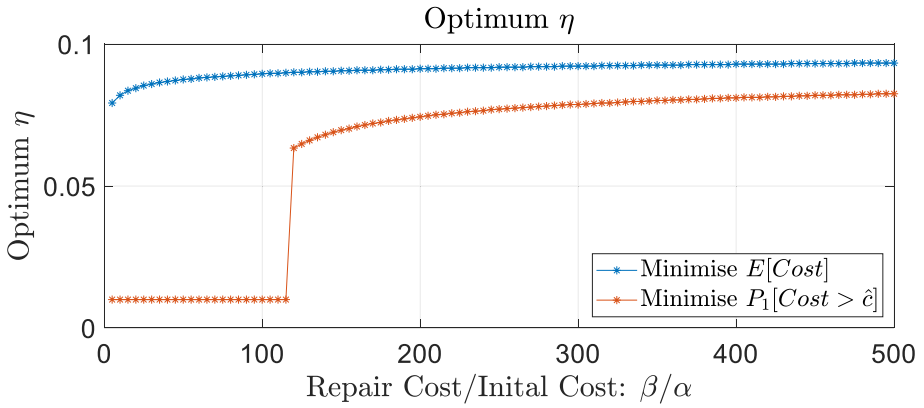

Fig. 16. Change in Optimal η value with the ratio of repair cost to initial cost,.β/α

show that theoretically the optimum value of η is different if $E[C]$ or $P_1[C > \widehat{c}]$ is minimised. Instead, at least for the computationally cheap models considered in this paper, it is more practical to evaluate $E[C]$ or $P_1[C > \widehat{c}]$ for a range of x and η values and extract the minimum value. This avoids challenges associated with numerical differentiation and also means that the cost function is not required to be strictly differentiable.

The difference between the two approaches is illustrated in Fig. 16, which shows the optimum η values obtained for a range of repair cost to initial cost, i.e. β/α in Eq. (11), ratios. From Fig. 16, it can be appreciated that the optimum η from the two methods is not the same, demonstrating numerically that employing the distinction between Probability_1 and Probability_2 can lead to different design decisions.

5. Limitations

The examples in the preceding sections are intended to be illustrative, and as has been already discussed, the computational models employed are excessively simple. In most realistic engineering dynamics problems more expensive computational models are required. Furthermore, this study only considers examples where the respective uncertainties derive from a single variable. In reality there are likely to be multiple parameters contributing to both forms of uncertainty, meaning that large multi-dimensional probability spaces need to be considered. Theoretically, there is no reason why the approach could not be expanded for this. However, as implemented here, doing so would require computationally expensive nested simulations. This computational expense may make some of the calculation procedures adopted here impractical and more sophisticated approaches, for example potentially using Latin Hypercube Sampling or surrogate modelling, are likely to be necessary to develop a response surface for real world, multi variable problems.

In addition, the examples are predicated on the assumption that a probability distribution can be defined for all uncertain parameters. In reality, the values that define the distribution will themselves be uncertain, adding an extra layer of complexity to the problem. However, it is possible to expand the framework outlined to deal with these uncertainties [16], although again it would likely require more sophisticated sampling in the development of conditional distributions.

Finally, the work is limited to a probabilistic view of epistemic uncertainty. There is ongoing debate about this in literature; some authors argue that this is correct (for example [3]), while others argue that probability theory is insufficient to model ignorance and that some form of imprecise probability should be employed. It may be possible to develop the framework to incorporate imprecise probability theory by developing a credal set of possible probability distributions to represent epistemic uncertainty and, in the one dimensional case then propagating upper and lower bounds through the framework. This is likely to be more difficult for the realistic multi-dimensional case.

6. Conclusion

Carnap argued that both subjective and frequentist views of probability are necessary and should be maintained as separate quantities, which he termed Probability_1 and Probability_2. These two definitions of probability broadly correspond to epistemic and aleatory uncertainty. This paper explores the benefits performing probabilistic analysis in engineering dynamics where aleatory and epistemic uncertainties are treated as distinct quantiles, in line with Carnap's ideas. Two metrics based on second order probability are examined to demonstrate the potential benefits of such an approach. It is argued that understanding the balance of reducible and irreducible uncertainties at the design stage allows design decisions to be made from a more informed position. Furthermore, understanding this balance is especially relevant when a digital twin approach is adopted given that one of the aims of a digital twin is to reduce this uncertainty. It is also shown that treating the uncertainty types separately can lead to different solutions in the selection of optimum design parameters. Therefore, it is concluded that as well as being more philosophically consistent than the conventional combining uncertainties, employing the two descriptions of probability is potentially valuable approach in engineering dynamics.

7. Data access

Additional data related to this publication is available at the 'Mendeley Data' data repository at the following link**:** https://data.mendeley.com/datasets/pjtn2nhnm2/draft?a = e62a163a-3661–4062-bbcd-86224e5dda96.

Funding

This work was funded by UKRI grant EP/R006768/1. For the purpose of open access, the author has applied a Creative Commons Attribution (CC BY) licence to any Author Accepted Manuscript version arising.

CRediT authorship contribution statement

John Hickey: Methodology, Software, Visualization, Writing – original draft. **Robin Langley:** Conceptualization, Writing – review & editing, Supervision, Funding acquisition.

Declaration of Competing Interest

The authors declare the following financial interests/personal relationships which may be considered as potential competing interests: John Hickey reports financial support was provided by Engineering and Physical Sciences Research Council.

Appendix A. Example sensitivity to choice of p_1 distribution

As discussed in Section 3 paper, the choice of a normal distribution to represent damping in the Tall Building example is illustrative, and is not necessarily be the best way to represent damping. This appendix examines the impact of changing this distribution from normal to uniform. The two distributions, and the associated $P_1[P_2]$ C-CDFs are compared in Fig. A.1. Firstly, on a basic level, the fact the framework is applicable in both cases illustrates that the method can work for any probability distribution. Secondly, for this example case it can be appreciated that while there are some differences, namely a slightly higher P_1 proability of encountering higher p_2 failure probabilities if a uniform distribution is employed, the C-CDF is not overly sensitive to this change. However, it is important to stress that this outcome is only applicable to this particular example problem and it is not valid to conclude that the proposed metric is insensitive to the choice of p_2 distribution in all cases or for all choices of distribution.

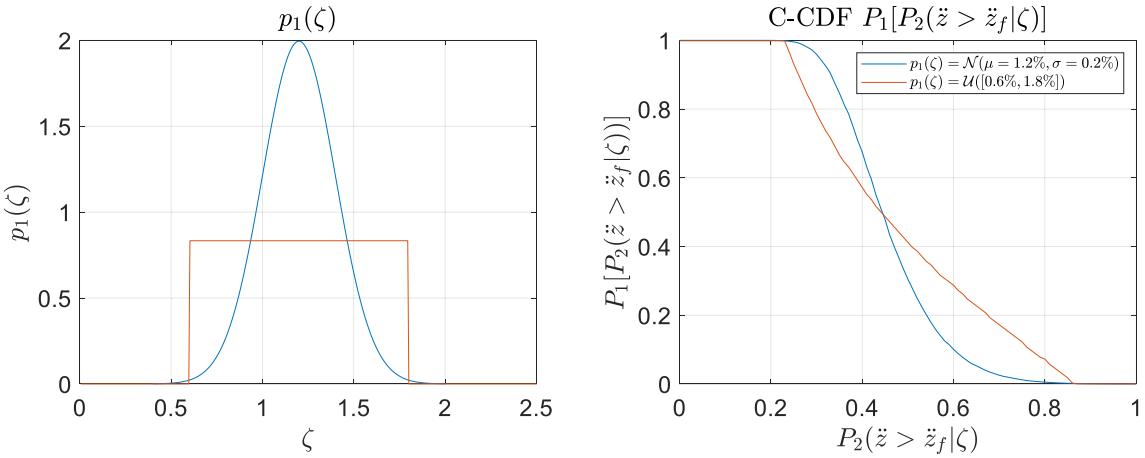

Fig. A1. Comparison of C-CDF for the tall building example problem using an example normal distribution (mean 1.2%, standard deviation 0.2%) and uniform distribution (U[0.6%, 1.8%]) for damping.

Appendix B. Proof

It can be shown that the area enclosed by the C-CDF of $P_1[P_2(\mathit{fail}) > \widehat{P}_2]$ is equal to the P_0 probability of failure calculated via Eq. (1). This can be shown by rewriting Eq. (3) using the Heaviside step function, H:

$$P_1\left[P_2\left(z > z_f\right) > \widehat{P}_2\right] = \int_{-\infty}^{\infty} \mathrm{H}\left[P_2\left(z > z_f|x\right) - \widehat{P}_2\right] p(x)\mathrm{d}x \tag{B1}$$

and integrating across the range of possible $\widehat{P}_2$ values (0 to 1) to find the area under the C-CDF:

$$\int_0^1 \left\{P_1\left[P_2\left(z > z_f\right) > \widehat{P}_2\right]\right\}\mathrm{d}\widehat{P}_2 = \int_0^1 \int_{-\infty}^{\infty} \mathrm{H}\left[P_2\left(z > z_f|x\right) - \widehat{P}_2\right] p(x)\mathrm{d}x\mathrm{d}\widehat{P}_2 \tag{B2}$$

For a given $P_2(\mathit{fail}|\boldsymbol{x})$ the integral of the Heaviside step function is:

$$\int_0^1 \mathrm{H}\left[P_2\left(z > z_f|x\right) - \widehat{P}_2\right]\mathrm{d}\widehat{P}_2 = P_2\left(z > z_f|x\right) \tag{B3}$$

Hence, Eq. (B.2) can be rewritten as:

$$\int_0^1 \left\{P_1\left[P_2\left(z > z_f\right) > \widehat{P}_2\right]\right\}\mathrm{d}\widehat{P}_2 = \int_{-\infty}^{\infty} P_2\left(z > z_f|x\right) p(x)\mathrm{d}x \tag{B4}$$

Substituting Eq. (2) into Eq. (B.4) gives:

$$\int_0^1 \{P_1[P_2(z > z_f) > \widehat{P}_2]\} d\widehat{P}_2 = \int_{-\infty}^{\infty} \int_{R_1} p_2(y) p_1(x) dy dx \tag{B5}$$

Which can be rewritten as a joint PDF of x and y, $p_{1,2}(x,y)$:

$$\int_0^1 \{P_1[P_2(z > z_f) > \widehat{P}_2]\} \mathrm{d}\widehat{P}_2 = \iint_{R(z>z_f)} p_{1,2}(x,y) \mathrm{d}x\mathrm{d}y \tag{B6}$$

which, by Eq. (1), is the P_0 failure probability with no distinction between uncertainty types:

$$\int_0^1 \{P_1[P_2(z > z_f) > \widehat{P}_2]\} \mathrm{d}\widehat{P}_2 = P_0(z > z_f | x, y) \tag{B7}$$

References

[1] A. Hájek, Interpretations of Probability, in: E.N. Zalta (Ed.), The Stanford Encyclopedia of Philosophy, Fall 2019, Metaphysics Research Lab, Stanford University, 2019. https://plato.stanford.edu/archives/fall2019/entries/probability-interpret/ (accessed December 6, 2021).

[2] G.B. King, A.E. Lovell, L. Neufcourt, F.M. Nunes, Direct Comparison between Bayesian and Frequentist Uncertainty Quantification for Nuclear Reactions, Phys. Rev. Lett. 122 (2019), 232502, https://doi.org/10.1103/PhysRevLett.122.232502.

[3] A. O'Hagan, Expert knowledge elicitation: subjective but scientific, Amer. Statist. 73 (2019) 69–81, https://doi.org/10.1080/00031305.2018.1518265.

[4] R. Carnap, Logical Foundations of Probability, Chicago, IL, Chicago University of Chicago Press, USA, 1950.

[5] M.I. Jyrkama, M.D. Pandey, On the separation of aleatory and epistemic uncertainties in probabilistic assessments, Nucl. Eng. Des. 303 (2016) 68–74, https://doi.org/10.1016/j.nucengdes.2016.04.013.

[6] Fema Seismic performance assessment of buildings (Second Edition), Implementation Guide", CA, USA: Applied Technology Council for the Federal Emergency Management Agency 2018.

[7] W.L. Oberkampf, J.C. Helton, C.A. Joslyn, S.F. Wojtkiewicz, S. Ferson, Challenge problems: uncertainty in system response given uncertain parameters, Reliab. Eng. Syst. Saf. 85 (2004) 11–19, https://doi.org/10.1016/j.ress.2004.03.002.

[8] A.D. Kiureghian, O. Ditlevsen, Aleatory or epistemic? Does it matter? Struct. Saf. 31 (2009) 105–112, https://doi.org/10.1016/j.strusafe.2008.06.020.

[9] J. Mullins, Y. Ling, S. Mahadevan, L. Sun, A. Strachan, Separation of aleatory and epistemic uncertainty in probabilistic model validation, Reliab. Eng. Syst. Saf. 147 (2016) 49–59, https://doi.org/10.1016/j.ress.2015.10.003.

[10] Y.H. Hou, Y.J. Li, X. Liang, Mixed aleatory/epistemic uncertainty analysis and optimization for minimum EEDI hull form design, Ocean Eng. 172 (2019) 308–315.

[11] S. Ferson, L.R. Ginzburg, Different methods are needed to propagate ignorance and variability, Reliab. Eng. Syst. Saf. 54 (1996) 133–144, https://doi.org/10.1016/S0951-8320(96)00071-3.

[12] J.C. Helton, J.D. Johnson, W.L. Oberkampf, C.J. Sallaberry, Representation of analysis results involving aleatory and epistemic uncertainty, Int. J. Gen Syst 39 (2010) 605–646, https://doi.org/10.1080/03081079.2010.486664.

[13] L.W. Cook, J.P. Jarrett, Horsetail matching: a flexible approach to optimization under uncertainty, Eng. Optim. 50 (2018) 549–567, https://doi.org/10.1080/0305215X.2017.1327581.

[14] J.C. Helton, C.J. Sallaberry, Conceptual basis for the definition and calculation of expected dose in performance assessments for the proposed high-level radioactive waste repository at Yucca Mountain, Nevada, Reliab. Eng. Syst. Saf. 94 (2009) 677–698, https://doi.org/10.1016/j.ress.2008.06.011.

[15] J.C. Helton, C.J. Sallaberry, Computational implementation of sampling-based approaches to the calculation of expected dose in performance assessments for the proposed high-level radioactive waste repository at Yucca Mountain, Nevada, Reliab. Eng. Syst. Saf. 94 (2009) 699–721, https://doi.org/10.1016/j.ress.2008.06.018.

[16] J.C. Helton, C.J. Sallaberry, Uncertainty and Sensitivity Analysis: From Regulatory Requirements to Conceptual Structure and Computational Implementation, in: A.M. Dienstfrey, R.F. Boisvert (Eds.), Uncertainty Quantification in Scientific Computing, Springer, Berlin, Heidelberg, 2012, pp. 60–77, https://doi.org/10.1007/978-3-642-32677-6_5.

[17] J.C. Helton, C.W. Hansen, C.J. Sallaberry, Expected dose for the nominal scenario class in the 2008 performance assessment for the proposed high-level radioactive waste repository at Yucca Mountain, Nevada, Nevada, Reliability Engineering & System Safety. 122 (2014) (2008) 267–271, https://doi.org/10.1016/j.ress.2013.06.012.

[18] P.N. Swift, C.W. Hansen, J.C. Helton, R.L. Howard, M. Kathryn Knowles, R.J. MacKinnon, J.A. McNeish, S. David Sevougian, performance assessment for the proposed high-level radioactive waste repository at Yucca Mountain, Nevada, Reliability Engineering & System Safety. 122 (2014) 449–456.

[19] J. Baron, Second-order probabilities and belief functions, Theor Decis. 23 (1987) 25–36, https://doi.org/10.1007/BF00127335.

[20] D. Wagg, K. Worden, R. Barthorpe, P. Gardner, Digital Twins: State-of-The-Art Future Directions for Modelling and Simulation in Engineering Dynamics Applications, ASCE-ASME J Risk and Uncert in Engrg Sys Part B Mech Engrg. 6 (2020), https://doi.org/10.1115/1.4046739.

[21] M.J. Glanville, K.C.S. Kwok, R.O. Denoon, Full-scale damping measurements of structures in Australia, J. Wind Eng. Ind. Aerodyn. 59 (1996) 349–364, https://doi.org/10.1016/0167-6105(96)00016-5.

[22] T. Kijewski-Correa, J. Kilpatrick, A. Kareem, D.-K. Kwon, R. Bashor, M. Kochly, B.S. Young, A. Abdelrazaq, J. Galsworthy, N. Isyumov, D. Morrish, R.C. Sinn, W. F. Baker, Validating Wind-Induced Response of Tall Buildings: Synopsis of the Chicago Full-Scale Monitoring Program, J. Struct. Eng. 132 (2006) 1509–1523, https://doi.org/10.1061/(ASCE)0733-9445(2006)132:10(1509).

[23] International Standards Organization, ISO 10137:2007 Bases for design of structures - Serviceability of buildings and walkways against vibrations, (2007). https://www.iso.org/cms/render/live/en/sites/isoorg/contents/data/standard/03/70/37070.html (accessed December 6, 2021).

[24] CEN, Eurocode 1: Actions on Structures–Part1-4: General actions-wind actions; EN 1991-1-4: 2005, Comite Europeen de Normalisation. (2005).

[25] R.D.J.M. Steenbergen, A.C.W.M. Vrouwenvelder, C.P.W. Geurts, The use of Eurocode EN 1991–1-4 procedures 1 and 2 for building dynamics, a comparative study, J. Wind Eng. Ind. Aerodyn. 107–108 (2012) 299–306, https://doi.org/10.1016/j.jweia.2012.03.025.

[26] M.S. Kompella, R.J. Bernhard, Measurement of the Statistical Variation of Structural-Acoustic Characteristics of Automotive Vehicles, SAE International, Warrendale, PA (1993), https://doi.org/10.4271/931272.

[27] R.S. Langley, A.W.M. Brown, The ensemble statistics of the energy of a random system subjected to harmonic excitation, J. Sound Vib. 275 (2004) 823–846, https://doi.org/10.1016/S0022-460X(03)00780-6.
[28] S. Donders, M. Brughmans, L. Hermans, N. Tzannetakis, The Effect of Spot Weld Failure on Dynamic Vehicle Performance, (n.d.) 19.
[29] R.H. Lyon, R.G. DeJong, Theory and Application of Statistical Energy Analysis, Butterworth-Heinemann, 1995.
[30] R.L. Weaver, On the ensemble variance of reverberation room transmission functions, the effect of spectral rigidity, J. Sound Vib. 130 (1989) 487–491, https://doi.org/10.1016/0022-460X(89)90071-0.
[31] P. Bertelsen, C. Ellegaard, E. Hugues, Distribution of eigenfrequencies for vibrating plates, Eur. Phys. J. B. 15 (2000) 87–96, https://doi.org/10.1007/s100510051102.
[32] R.S. Langley, J. Legault, J. Woodhouse, E. Reynders, On the applicability of the lognormal distribution in random dynamical systems, J. Sound Vib. 332 (13) (2013) 3289–3302.
[33] P.J. Shorter, R.S. Langley, Vibro-acoustic analysis of complex systems, J. Sound Vib. 288 (2005) 669–699, https://doi.org/10.1016/j.jsv.2005.07.010.